

Influence of geotextile encasement on the behaviour of stone columns:

Laboratory study

by

Marina Miranda (1) (*) (+), Almudena Da Costa (2), Jorge Castro (3), César Sagasetta (4)

Group of Geotechnical Engineering

Department of Ground Engineering and Materials Science

University of Cantabria

Avda. de Los Castros, s/n

39005 Santander, Spain

Tel.: +34 942 201813

Fax: +34 942 201821

e-mail: (1) M.Miranda@napier.ac.uk; (2) dacostaa@unican.es; (3) castrogj@unican.es;

(4) sagasetac@unican.es

(*) Corresponding Author

(+) Affiliation: Edinburgh Napier University (formerly University of Cantabria)

School of Engineering and the Built Environment,

Edinburgh Napier University,

10 Colinton Road, Edinburgh EH10 5DT, UK

Date: March 2016

ABSTRACT

This paper presents a study of the influence of the geotextile encasement on the behaviour of soft soils improved with fully penetrating encased columns. This influence is analyzed by means of measuring soil-column stress distribution, pore pressures and soil deformation during the consolidation process. For this purpose, a horizontal slice of a representative "unit cell" has been analysed by means of small-scale laboratory tests. The tests were carried out in a large instrumented Rowe-Barden oedometric cell. Results showed that the vertical stress supported by encased columns is about 1.7 times that sustained by the non-encased ones. The stress concentration factor for encased columns is between 11 and 25, which is clearly higher than that obtained in tests with non-encased columns, which are between 3 and 6. Finally, the improvement in relation to settlements is presented by the ratio of settlement in soils reinforced with ordinary or encased columns and the settlement of non-treated soft soil. This settlement reduction factor is around 0.6 when the soil is treated with encased columns and 0.8 for soil with non-encased columns.

KEYWORDS: Geosynthetics, small-scale test, soft soil, settlement reduction, stress concentration factor, encased-columns.

Introduction

Encased stone columns are widely employed in very soft soils ($s_u < 15 \text{kPa}$) to improve bearing capacity, to reduce settlements and to increase the speed of consolidation. Columns act as relatively rigid and permeable inclusions in the soft soil allowing for the reduction of settlements, the increase of bearing capacity, and the reduction of time needed for consolidation. The effectiveness of its performance is mainly based on the soil-column load distribution, which largely depends on the lateral support provided by the soft soil. In very soft soils, with undrained shear strengths lower than some limit

between 15 and 5 kPa (Wehr, 2006), this lateral support is not sufficient, and columns may fail because of excessive bulging (McKenna et al., 1975). In these situations, one widely employed solution to enhance the performance of this treatment is to wrap the columns with a geosynthetic encasement. The main advantages of encased columns compared to ordinary columns are the extra lateral support provided by the geotextile encasement, and stopping fine particles of the soft soil squeezing inside the column avoiding clogging. This technique has been successfully employed in foundations of roads and railways under embankments (Raithel et al., 2005).

The use of encased stone columns among the last decades has come with an increase in studies performed to analyse their behaviour. One of the first attempts was presented by Van Impe (1989). Since then, several analytical studies have been developed such as Castro and Sagaseta (2011, 2013), Pulko et al. (2011) and Raithel and Kempfert (2000). In addition to analytical research, several numerical studies have been performed. Some of them presented parametric studies focused on the influence of the stiffness of the geotextile encasement (e.g., Almeida et al., 2013; Malarvizhi and Ilamparuthi, 2007; Murugesan and Rajagopal, 2006) or on the influence of the encasement length (e.g., Dash and Bora, 2013). Most of the numerical studies have been performed using 2D simulation but there are also some 3D approaches (e.g., Keykhosropur et al., 2012; Lo et al., 2010, Yoo, 2015 and Yoo and Kim, 2009).

Numerous experimental studies related to encased columns have also been developed. Full-scale tests were performed in several analyses (e.g., Alexiew et al., 2009; Almeida et al., 2015; Chen et al. 2015; Hosseinpour et al. 2015; Raithel et al., 2002 and Yoo and Lee, 2012), although small-scale laboratory tests were carried out in most of the studies. In these last cases the column diameter is significantly smaller than that in real treatments and the geotextile sleeves are generally formed by a flat fabric with a longitudinal joint;

however, continuous sleeves are usually employed in real treatments. This joint in laboratory tests is commonly made by an overlap of the fabric, which can be sewn (e.g., Hong, et al. 2016; Murugesan and Rajagopal, 2007, 2010) or it can be glued (e.g., Ghazavi and Afshar, 2013 and Gniel and Bouazza, 2009, 2010). This results in a weak point that reduces the strength of the geotextile (Alexiew et al. 2012). The majority of these experimental studies focus on the load-settlement response (e.g., Gniel and Bouazza, 2009; Murugesan and Rajagopal, 2007, 2010).

The objective of this research is to analyse the influence of the encasement on stone columns by means of small-scale laboratory tests. The main novelty of this research is the analysis of settlements, total stresses and pore water pressures not only for drained conditions but also during the whole consolidation process. This is accomplished by performing experimental laboratory tests in a large diameter oedometric cell. The research is focused on soil-column stress distribution, settlements and pore pressure dissipation in soft soils treated with encased columns. In addition, the improvement achieved when the stone column is encased with a geotextile is compared with non-encased columns.

Experimental set-up

In real treatments under large uniformed loaded areas, stone columns are installed forming meshes of regular patterns (triangular, hexagonal or square). A widely employed simplification for their analysis is the consideration of one single column and its corresponding surrounding soil which is referred to as "unit cell". The laboratory tests were designed to study fully penetrating encased columns, neglecting tip effects, with no influence of the column length and only radial drainage. This allows simplifying the analysis to a slice of a "unit cell" at a certain depth. For this purpose, small-scale laboratory tests were performed in a Rowe-Barden oedometric cell (Rowe and Barden,

1966), 254 mm in diameter and 146 mm height. The geometry of the unit cell was defined by a diameter ratio of $N=3$ (N , ratio between diameter of the elementary cell and column diameter). This corresponds to a column diameter of 84.7mm and to an area replacement ratio of $a_r=11\%$, resulting a scale of the tests about 1/10 respect to real cases. Regarding the boundary conditions, only radial drainage towards the column was allowed and equal strain condition was simulated by placing a rigid plate on the top surface.

The oedometric cell was instrumented focussing on the study of column-soil stress distribution, pore pressure dissipation and measurement of the rate of strains during the consolidation process. With this aim 6 pore pressure transducers (PPT) and 7 total stress transducers (TST) were allocated in the base of the oedometric cell. Total stresses under the column were measured by three TST (XPM10-50G-HA-LC1, QBM, pressure cells 8 mm in diameter) placed in a triangular pattern, at 22.5 mm from the centre of the cell. Total stresses on the soil were measured by 4 TST (XPM10-10G-LC1, QBM, pressure cells 8 mm in diameter) which were placed at different distances from the centre ($r=49, 58, 69$ and 115 mm). Pore pressures (WF17060, Wykeham Farrance, pressure cells 4 mm in diameter) were also measured at different distances from the centre ($r=49, 53, 58, 69, 84.5$ and 115 mm). Figure 1 shows the instrumented base. Two horizontal TST (XPM10-10G-LC1, QBM, pressure cells 8 mm in diameter) were placed diametrically opposed in the lateral boundary of the cell at 20 mm height from the base to measure horizontal stresses on the soil. Finally a LVDT was set up at the central point on the top of the cell to measure vertical displacements. More details of the instrumentation can be found in Cimentada, 2009 and Miranda, 2014.

Characterization of the materials

Kaolin clay was employed as soft soil, limestone gravel for the column and two different geotextiles as encasements.

Relevant properties of the kaolin, obtained from laboratory tests, are summarised in TABLE 1 (Cimentada et al. 2011).

Uniform gravel with particle sizes between 4 and 5 mm was used for the column, according to the 1/10 scale of the test. The maximum and minimum dry unit weights are 16.5 and 13 kN/m³, which correspond to void ratios of $e_{min}=0.64$ and $e_{max}=1.06$ respectively. A relative density of 50% was chosen to form the column which corresponds to a dry unit weight of 14.5kN/m³. Conventional drained triaxial tests were performed to obtain the values of the internal friction angle (ϕ) and the dilatancy angle (ψ). A summary of the most relevant properties of the gravel obtained from these tests is given in TABLE 2. Laterally confined stress path-controlled drained triaxial tests were also carried out to obtain the oedometric modulus of the gravel resulting in a value of $E_{mc}=20000$ kPa.

Two different geotextiles were employed to encase the column; both of them were provided by Huesker Synthetic Gmb and made using a different flat fabric. In both cases the fabric was cut and prepared in a cylindrical shape; hence a longitudinal joint was needed to form the sleeve.

Geotextile1 fabric is Stabilenca 120/120, which is formed by longitudinal and transversal polyester threads. Its design tensile strength is 120 kN/m. The longitudinal joint was formed by an overlap of 2 cm of the fabric that was glued with an epoxy adhesive.

Geotextile2 fabric is Robutec 130/25, which is formed by threads of polyvinyl alcohol in longitudinal direction and polypropylene threads in the transverse direction. Its design transversal tensile strength is 130 kN/m. The longitudinal joint was made in the same manner as for geotextile1.

Tensile strength tests were performed by Huesker Synthetic Gmb for both fabrics and both geotextiles (fabric+joint) following the standards DIN EN ISO 10319 and DIN EN ISO 10321, respectively. All of the tests were performed on 200 mm wide samples

(similar dimension to the circumferential length of 266 mm of the encasements employed for the tests). The results of these tests are shown in Figure 2 and the values of the secant modulus obtained from them are given in TABLE 3 and TABLE 4 for geotextile1 and geotextile2, respectively.

The behaviour of the gravel encased with these geotextiles was analysed by triaxial drained tests (Miranda and Da Costa, 2016).

Sample preparation

Sample preparation involved the preparation of the kaolin clay bed and the installation of the central encased column. Remoulded kaolin clay consolidated under 50 kPa was used as clay bed. First, the kaolin clay was mixed with a water content of 1.5 times its liquid limit, then it was poured into the Rowe-Barden cell and finally, it was consolidated under 50 kPa. Under this pressure the undrained shear strength of the kaolin clay is about 12 kPa, value in the range for treatment with encased columns.

The column was prefabricated with the aid of a nylon mould. In cases of encased columns, the geotextile was placed inside the mould and the required quantity of gravel needed to achieve the desired density (14.5 kN/m^3 dry unit weight) was placed inside the mould. Afterwards, it was saturated with water and left to freeze for at least 48 hours. Finally, the column was taken out of the nylon mould and placed in a pre-bored central hole. Once the column was placed, it was left to thaw, and the sample surface was levelled. Finally, the soil-column sample was consolidated again under 50 kPa. This method of column installation does not represent the real one but makes the repeatability of the tests easier. In addition, it has been successfully employed in previous studies (Cimentada et al., 2011; Gniel and Bouazza, 2009 and 2010; Miranda et al., 2015 or Sivakumar et al., 2004).

Test procedure

Each test consisted in three vertical stress increments, 50 kPa for the first one and 100 kPa for the other two, reaching a final vertical stress of 300kPa. Each vertical stress increments started with the application of the load under undrained conditions. Once the excess of pore pressure reached the value of the applied load, the drainage was allowed and the consolidation process took place for 24 hours. To avoid problems with the air trapped into the soil, a back pressure of 300 kPa was set during the whole test. To interpret the results, this back pressure has been subtracted from the measurements.

Three different series of tests were performed, each one using a different type of column: encased columns with geotextile1, encased columns with geotextile2 and non-encased columns. Each series consisted of 3 or 4 equal tests to ensure repeatability.

Results and discussion

Results obtained from the tests with encased and non-encased columns are compared in this section to analyse the influence of the geotextile encasement. The obtained results are presented focusing on soil-column stress distribution, reduction of settlements, and dissipation of pore pressures.

Measurements were obtained for the three load steps in each of the 10 performed tests. In the following, to make the analysis of the results clear, average values of tests performed with the same characteristics were employed. This average was considered since results show good repeatability, as it can be seen in Figure 3.

Vertical stresses

Soil-column stress distribution is one of the main features of soft soils improved with encased stone columns. Vertical load supported by the natural soil decreases due to the transfer of part of the applied load to the column. The stress on the column was calculated

as the average of the readings in the three sensors located under the column, while the stress on the soil was obtained as the average, weighted with the influence area, of each of the sensors located under the soil.

Values of the stresses on the soil and on the column during the consolidation process are presented in Figure 4 and Figure 5, respectively. In both figures, the stresses are given as the ratio of the increment in the soil and column vertical stresses from the beginning of the step ($\Delta\sigma_{zs}, \Delta\sigma_{zc}$), to the increment of the total applied pressure ($p_a=50$ kPa in the first load step and $p_a=100$ kPa in the second and third ones). The tendency is the same for the three series of tests (encased with geotextile1, encased with geotextile2 and non-encased). The results show that at the beginning of a load step, all of the applied pressure is nearly equally supported by the soil and the column. With time, soil behaviour changes from undrained (no volume change and therefore high stiffness) to drained behaviour (the soil becomes softer). Regarding the influence of the encasement, the stresses supported by encased columns are higher than the stresses on the non-encased columns. This is attributed to the extra lateral support provided by the geotextile and therefore the higher stiffness of the encased columns. Comparing the two encasements, the load transmitted to the column is similar in both cases, with slightly lower values with geotextile2. This is in agreement with the lower stiffness of this geotextile in the low range of radial strains developed during the test (1 to 3%).

Stresses on the soil and column at the end of each load step are shown in Figure 6 for both, column and soil. The results show the great influence of the encasement on the same way as previously presented. The encasement generates an increase in the stresses supported by the column, with values of the stresses on encased columns around 1.7 times the stresses on non-encased columns. In addition, there is a decrease in the stresses on the

soil with values for samples with encased columns between 0.5 and 0.7 times the stresses on the soil in tests with non-encased columns.

Small differences between the values obtained for both encasements can be observed in the first two load steps (in agreement with the lower stiffness of the geotextile2 in the range of 1 to 3% vertical stains developed during the tests). However, in the third load step these differences are higher showing a noticeable decrease in the stresses on the column encased with geotextile2. This is associated to the partial breakage of the longitudinal joint, which is due to a worse behaviour of the adhesive with the fabric of geotextile2. In these cases the joint was found partially broken at the end of the test (Figure 7). This degradation of the joint is mean to be progressive achieving the breakage just in the last load step.

Stress concentration factor

The transfer of load between the column and the soil is usually expressed by means of the stress concentration factor (*SCF*), ratio between the total vertical stress on the column and on the soil. To analyse each load step independently, the incremental *SCF* defined as $\Delta\sigma_{zc}/\Delta\sigma_{zs}$ has been used. Final drained values of the *SCF* at the end of each load step, for all of the performed tests, are given in TABLE 5. There is some scatter in the results caused by the readings in the transducers located under the column, as usually happens in granular materials. Nevertheless, the trend and the obtained average values are clear. The values obtained for the non-encased columns are between 6 and 3, within the usual range of 3-10 presented by Barksdale and Bachus (1983). The *SCF* values related to encased columns are higher, being in the range of 11 to 25 (disregarding the low values in the last load step in tests with geotextile2 because of the breakage of the joint of the geotextile). The values obtained for the two encasements are similar for the first two load steps, being

lower the ones of tests performed with geotextile 2. This is due to the lower stiffness of this geotextile at low strains. In the last load step the difference is higher due to the partial breakage of the joint in cases with geotextile2.

Average values of the incremental *SCF* at the end of each load step for encased and non-encased columns are plotted in Figure 8. The trend is clear, the *SCF* decreases with increasing loads due to the development of plastic strains in the column. The *SCF* values obtained in the tests with encased columns are between 2.5 and 4.5 times those obtained in the tests with ordinary columns, which is in accordance with the higher stiffness of the encased columns.

The development of the *SCF* during the consolidation process is plotted in Figure 9 for the second load step. At the beginning of the stress increment the load is equally supported by the soil and the column. At this initial point the behaviour of the soil is undrained, with no volume change and therefore stiffer soil, but with time the soil drains and the load is transferred to the column. During this process of consolidation the stiffness of the soil decreases and the column is stiffer than the drained soil. This load transfer occurs until the column achieves its active state and no more load transfer takes place. The trend is similar for encased and non-encased tests, but a higher load transfer in tests with encased columns can be observed.

Horizontal stresses in the soil

Horizontal stresses in the soil were also analysed from the measurements taken at the sensors located in the cell lateral boundary. The values during the consolidation process are shown in Figure 10. The trend is the same as previously presented for the vertical stresses in the soil. They decrease with time as the load is transferred to the column. Average final values at the end of each load step are given in Figure 11. Regarding the

influence of the geotextile, horizontal stresses in tests with encased columns are around 30% lower than those obtained in those with non-encased columns. The same behaviour can be observed for vertical stresses (Figure 4), since the geotextile encasement provides part of the lateral stresses in the soil-column contact. Comparing both geotextiles, the values in samples with geotextile1 are slightly lower than those for geotextile2, which is in agreement with the results of vertical stresses on the soil.

Settlements

The decrease in the vertical stress on the soil due to the presence of the columns, leads to a reduction of settlements. Axial strains during the consolidation process are presented in Figure 12. The measurements show that the reduction of settlements is higher when the column is encased, which is in agreement with the extra lateral support provided by the geotextile.. The reduction of settlements achieved by this treatment is usually expressed by the settlement reduction factor, ratio between the settlement with and without columns, ($\beta = s_z/s_{z0}$) or its inverse, the improvement factor (n). The settlement reduction factor for each load step was obtained dividing the vertical strain in tests with column by the vertical strain in a reference test with only kaolin, both for the same applied load. Values of the settlement reduction factor at the end of each load step are presented in Figure 13. Average final values at the end of the tests are: 0.58 in tests with columns encased with geotextile1, 0.62 for tests with geotextile2 and 0.77 for non-encased tests. This means that the reduction of settlements with the encased columns is around 40%, and around 30% for non-encased columns. Comparing both encasements, the values are quite similar, slightly lower for geotextile1, in agreement with the values of the *SCF* presented previously.

Pore pressures

The acceleration of the consolidation process is another of the main features of the treatment with stone columns. The dissipation of the excess pore pressures during the consolidation process is presented in Figure 14. It is plotted as the ratio of the increment of pore pressures at the beginning of the load step, to the initial increment (100 kPa). Curves have been plotted for encased and non-encased columns. A curve obtained with Barron's solution using the coefficient of consolidation of the kaolin for the range 100-200 kPa has been included. This curve shows the process of consolidation in the case of kaolin with drains (zero stiffness). The results show the high improvement achieved, in terms of faster consolidation, by using stone columns compared with the case of drains (Barron's solution). Comparing the results for non-encased and encased columns, it can be observed that the geotextile encasement increases the speed of consolidation even more.

The analytical solutions for the consolidation around stone columns use the same classical solution as for vertical drains but including the influence of the column stiffness through a modified consolidation coefficient. In this case, this equivalent coefficient of consolidation, c_{vr}^{eq} , represents the radial consolidation neglecting the vertical one. This parameter has been derived from the measurements of settlements in the tests, using the inflection point method proposed by Robinson (1997). Figure 15 shows the obtained values. This values are presented as the ratio of the equivalent coefficient of radial consolidation to the coefficient of consolidation of the kaolin clay obtained from an oedometric test ($c_v = 2.16 \text{ m}^2/\text{day}$). The results show that the dissipation of pore pressures is around 3 or 2 times quicker in samples with encased columns than that in the case of considering radial consolidation but with drains. The values obtained for geotextile1 are slightly higher than those for geotextile2. The influence of the encasement can also be

observed as the values for encased columns are slightly higher (around 1.3 times) than those obtained in tests with non-encased columns.

Conclusions

Three series of tests (one with non-encased columns and the other two with two different geotextile encasements) were examined. The results show the high influence of the encasements employed on the soil-column stress distribution. Encased columns support a vertical stress of around 1.7 times the vertical stress supported by the ordinary columns. Consequently, vertical stresses on the soil are lower in samples with encased columns. These differences in the stress distribution lead to higher values of the stress concentration factor in samples with encased columns. The results show that the values of the *SCF* in drained situations and in samples with encased columns are between 11 and 25 and in cases of non-encased columns are between 3 and 10. Therefore, the *SCF* in encased columns is around 2 to 4 times the *SCF* in non-encased columns. In samples with encased columns horizontal stresses on the soil are around 30% lower than those with ordinary columns.

The settlement reduction factor obtained at the end of the tests is 0.58 and 0.62 for columns encased with geotextile1 and geotextile2 respectively, and 0.77 for non-encased columns.

The acceleration of the consolidation process is noticeable, with pore pressures that dissipate around 1.3 times quicker in samples with encased stone columns than in those with non-encased columns.

Comparing the two employed encasements, the behaviour is quite similar, according with the similar stiffness of both geotextiles at low radial strains. Slightly higher differences appear at the end of the tests, which is attributed to the partial breakage of the longitudinal

joint in geotextile 2 due to the worse behaviour of the adhesive with the fabric of this geotextile.

Acknowledgments

The presented work is part of the research project “An integrated calculation procedure for stone columns, considering the influence of the method of installation”, for the Spanish Ministry of Science and Innovation (Ref.: BIA2009-13602). The first author also received a grant from the Spanish Ministry of Science and Innovation (BES-2010-032866). The authors would like to thank HUESKER Synthetic GmbH Company, in particular Ignacio Diego, for providing the geotextiles needed for the encasement and their properties.

References

- Alexiew, D., Moormann, C., Jud, H., 2009. Foundation of a coal/coke stockyard on soft soil with geotextile encased columns and horizontal reinforcement. In: Proc. 17th Int. Conf. on Soil Mech. Geotech. Eng., Alexandria, Egypt, pp. 2236–2239.
- Alexiew, D., Raithel, M., Kuster, V., Detert, O., 2012. 15 years of experience with geotextile encased granular columns as foundation system. In: Proc. Int. Symp. on Ground Improvement IS-GI, ISSMGE TC211, Brussels. Vol. IV, IV-3.
- Almeida, M. S. S., Hosseinpour, I., Riccio, M., 2013. Performance of a geosynthetic-encased column (GEC) in soft ground: Numerical and analytical studies. *Geosynthetics International*. 20 (4), 252-262.
- Almeida, M., Hosseinpour, I., Riccio, M., Alexiew, D., 2015. Behavior of geotextile-encased granular columns supporting test embankment on soft deposit. *J. Geotech. Geoenviron. Eng.*, 141(3), 04014116.

- Barksdale, R.D., Bachus, R.C., 1983. Design and construction of stone columns. Report FHWA/RD-83/026. National Technical Information Service, Springfield, Virginia.
- Castro, J., Sagaseta, C., 2011. Deformation and consolidation around encased columns. *Geotext. Geomembr.* 29 (3), 268-276.
- Castro, J., Sagaseta, C., 2013. Influence of elastic strains during plastic deformation of encased stone columns. *Geotext. Geomembr.* 37(4), 47-53.
- Chen, J. F., Li, L. Y., Xue, J. F., Feng, S. Z. 2015. Failure mechanism of geosynthetic-encased stone columns in soft soils under embankment. *Geotext. Geomembr.* 43(5), 424-431.
- Cimentada, A. 2099. Análisis experimental en modelo reducido de la consolidación radial y deformación de un suelo blando mejorado con columnas de grava. PhD dissertation. Spain. University of Cantabria.
- Cimentada, A., da Costa, A., Cañizal, J., Sagaseta, C. 2011., Laboratory study on radial consolidation and deformation in clay reinforced with stone columns. *Can. Geotech. J.* 48(1), 36-52.
- Dash, S. K., Bora, M. C., 2013. Influence of geosynthetic encasement on the performance of stone columns floating in soft clay. *Can. Geotech. J.* 50(7), 754–765.
- DIN EN ISO 10319, 1999. Geosynthetics - Wide Width Test of Geotextiles.
- DIN EN ISO 10321, 2008 Geosynthetics - Tensile test for joints/seams by wide-width strip method.
- Ghazavi, M., Afshar, J.N., 2013. Bearing capacity of geosynthetic encased stone columns. *Geotext. Geomembr.* 38, 26–36.
- Gniel, J., Bouazza, A., 2009. Improvement of soft soils using geogrid encased stone columns. *Geotext. Geomembr.* 27(3), 167–175.

- Gniel, J., Bouazza, A., 2010. Construction of geogrid encased stone columns: A new proposal based on laboratory testing. *Geotext. Geomembr.* 28(1), 108–118.
- Hong, Y.S., Wu, C.S., Yu, Y.S., 2016. Model tests on geotextile-encased granular columns under 1-g and undrained conditions. *Geotext. Geomembr.* 44 (1) 13-27.
- Hosseinpour, I., Almeida, M. S. S., Riccio, M., 2015. Full-scale load test and finite-element analysis of soft ground improved by geotextile-encased granular columns. *Geosynth. Int.* 22(6), 428-438.
- Keykhosropur, L., Soroush, A., Imam, R., 2012. 3D numerical analyses of geosynthetic encased stone column. *Geotext. and Geomembr.* 35, 61–68.
- Lo S.R., Zhang R., Mak J., 2010. Geosynthetic-encased stone columns in soft clay: A numerical study. *Geotext. and Geomembr.* 28(3), 292–302.
- Malarvizhi, S.N., Ilamparuthi, K., 2007. Comparative study on the behavior of encased stone column and conventional stone column. *Soils and Foundations.* 47 (5), 873-885.
- McKenna, J. M., Eyre, W. A., Wolstenholme, D. R., 1975. Performance of an embankment supported by stone columns in soft ground. *Geotechnique.* 25(1), 51–59.
- Miranda, M. 2014. Influencia de la densidad y del confinamiento con geotextil en columnas de grava. PhD dissertation. Spain. University of Cantabria.
- Miranda, M., Da Costa, A., 2016. Laboratory analysis of encased stone columns. *Geotext. and Geomembr.* 44(3), 269-277.
- Miranda, M., Da Costa, A., Castro, J., Sagasetta, C., 2015. Influence of gravel density in the behaviour of soft soils improved with stone columns. *Can. Geotech. J.* 52(12), 1968-1980.
- Murugesan, S., Rajagopal, K., 2006. Geosynthetic-encased stone columns: numerical evaluation. *Geotext. Geomembr.* 24 (6), 349-358.

- Murugesan, S., Rajagopal, K., 2007. Model test son geosynthetic-encased stone columns. *Geosynthetics Int.* 14 (6), 346-354.
- Murugesan, S., Rajagopal, K., 2010. Studies on the behavior of single and group of geosynthetic encased columns. *J. Geotech. Geoenviron. Eng.* 136 (1), 129-139.
- Pulko, B., Majes, B., Logar, J., 2011. Geosynthetic-encased stone columns: Analytical calculation model. *Geotext. and Geomembr.* 29(1), 29-39.
- Raithel, M., Kempfert, H. G., 2000. Calculation models for dam foundations with geotextile coated sand columns. In: *Proc. Int. Conf. on Geotechnical and Geological Engineering Geo Eng 2000*, Melbourne.
- Raithel, M., Kempfert, H. G., Kirchner, A., 2002. Geotextile encased columns (GEC) for foundation of a dike on very soft soils. In: *Proc. 7th Int. Conf. on Geosynthetics*, Nice, France, pp. 1025-1028.
- Raithel, M., Kirchner, A., Schade, C., Leusink, E., 2005. Foundation of Constructions on Very Soft Soils with Geotextile Encased Columns - State of the Art. *Innovations in Grouting and Soil Improvement*, pp. 1-11.
- Robinson, R.G., 1997. Determination of radial coefficient of consolidation by the inflection point method. *Geotechnique* 47(5), 1079-1081.
- Rowe, P.W., Barden, L., 1966. A new consolidation cell. *Géotechnique*, 16(2), 162-170.
- Sivakumar, V., McKelvey, D., Graham, J., Hughes, D., 2004. Triaxial tests on model sand columns in clay. *Canadian Geotechnical Journal*, 41(2), 299-312.
- Van Impe, W. F., 1989. *Soil improvement techniques and their evolution*. Balkema, Rotterdam, Netherlands.
- Wehr J., 2006. The undrained cohesion of the soil as criterion for the column installation with depth vibrator. In: *Proc. of the Int. Symposium on vibratory pile driving and deep soil vibratory compaction, TRANSVIB*, Paris.

- Yoo, C. 2015. Settlement behavior of embankment on geosynthetic-encased stone column installed soft ground—A numerical investigation. *Geotext. and Geomembr.*, 43(6), 484-492.
- Yoo, C., Kim, S.B., 2009. Numerical modelling of geosynthetic-encased stone column-reinforced ground. *Geosynthetics Int.* 16(3), 116–126.
- Yoo, C., Lee, D. 2012. Performance of geogrid-encased stone columns in soft ground: full-scale load tests. *Geosynthetics Int.* 19(6), 480-490.

FIGURE CAPTIONS

Figure 1. Instrumented base of the Rowe-Barden cell

Figure 2. Tensile force versus strain of the geotextiles.

Figure 3. Normalized vertical stresses on the soil with time (encased columns).

Figure 4. Normalized mean vertical stresses in the soil with time.

Figure 5. Normalized mean vertical stresses in the column with time.

Figure 6. Vertical stresses on the soil and on the column under drained conditions.

Figure 7. Encased column with geotextile2 at the end of the test.

Figure 8. Incremental *SCF* in drained situation.

Figure 9. Incremental *SCF* with time for the three load steps.

Figure 10. Horizontal stresses in the soil with time.

Figure 11. Horizontal stresses on the soil under drained conditions.

Figure 12. Axial strains with time.

Figure 13. Settlement reduction factor at the end of each load step.

Figure 14. Pore pressure with time.

Figure 15. Equivalent coefficient of consolidation using Robinson (1997) method.

TABLE 1. Properties of the kaolin clay (Cimentada et al., 2011)

Liquid limit [%]	73
Plastic limit [%]	38
Plasticity index	35
c_v [cm ² /s]	$2.5 \cdot 10^{-3} (*)$
C_c	0.53
C_s	0.10
e (50 kPa)	1.529
s_u/σ'_v (C-U triaxial tests)	0.30
ϕ [°] (C-U triaxial tests)	26.5

(*) range from 1.9 to $2.7 \cdot 10^{-3}$ cm²/s

TABLE 2. Results of triaxial tests on the gravel

	Sample 1	Sample 2	Sample 3
p'_0 [kPa]	50	150	300
ϕ [°]	47	42	39
Ψ [°]	15	5	0
ν	0.25	0.16	0.15
E_{50} [MPa]	5.96	12.68	16.03

p'_0 : confining stress

TABLE 3. Tensile strength and stiffness of the geotextile1with joint

Strain [%]	Tensile force [kN/m]	Secant modulus J_g [kN/m]
2	13	650
5	31	620
8	50	625
Max 12.3	77	626

TABLE 4. Tensile strength and stiffness of the geotextile2 with joint

Strain [%]	Tensile force [kN/m]	Secant modulus J_g [kN/m]
2	10	500
5	31	620
8	60	750
Max 8.7	67	770

TABLE 5. Values of the incremental *SCF* at the end of each load step

Vertical stress [kPa]		100	200	300
GTEX1	Test1	<i>45.6</i>	18.5	10.5
	Test2	14.3	14.4	8.7
	Test3	21.5	18.6	11.0
	Test4	25.6	21.1	15.7
	Average	20.5	18.2	11.5
GTEX2	Test1	15.8	18.3	6.2
	Test2	16.2	12.6	6.0
	Test3	18.1	8.6	5.7
	Average	16.7	13.2	6.0
Non-Encased	Test1	5.6	3.8	3.3
	Test2	5.4	3.5	3.5
	Test3	9.5	5.3	5.7
	Average	6.8	4.2	4.2

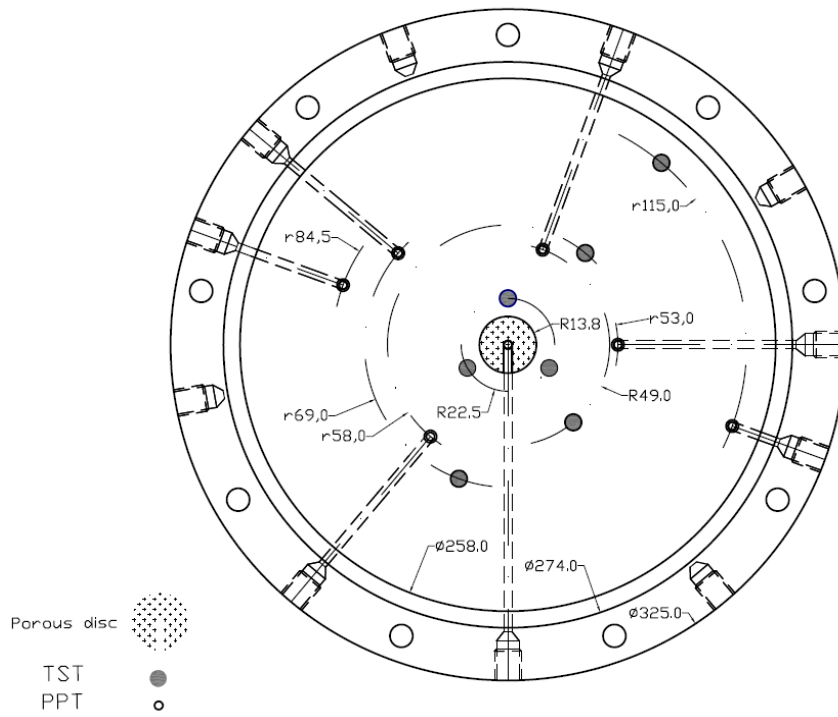


Figure 1. Instrumented base of the Rowe-Barden cell

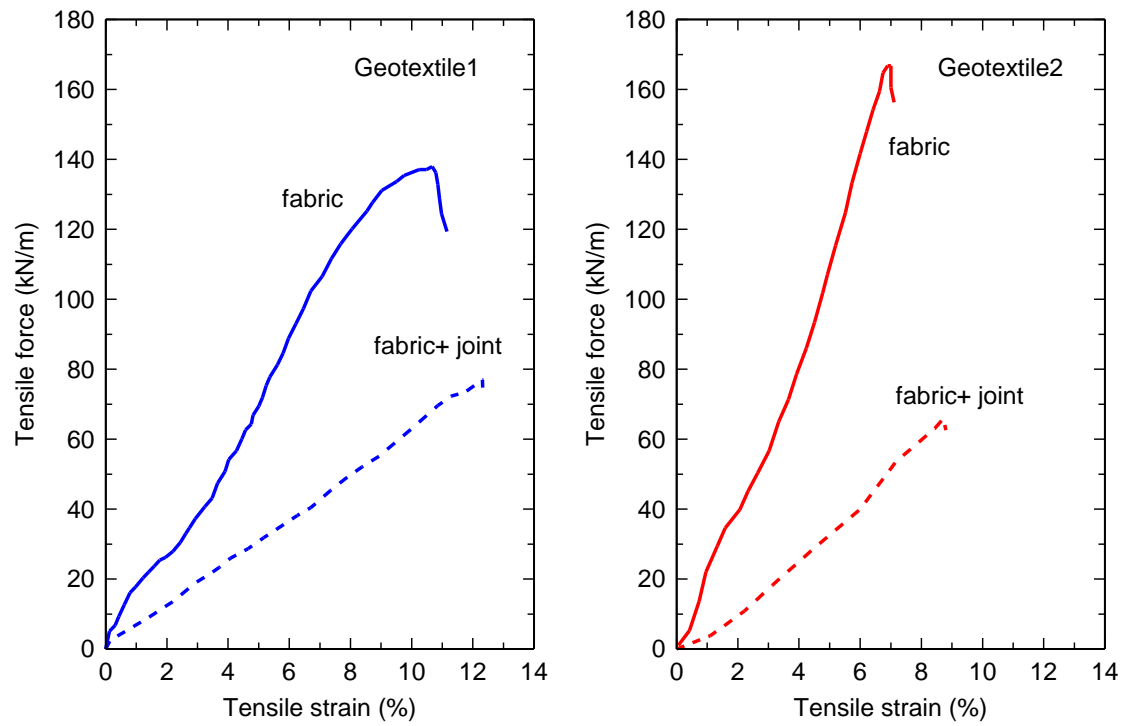


Figure 2. Tensile force versus strain of the geotextiles.

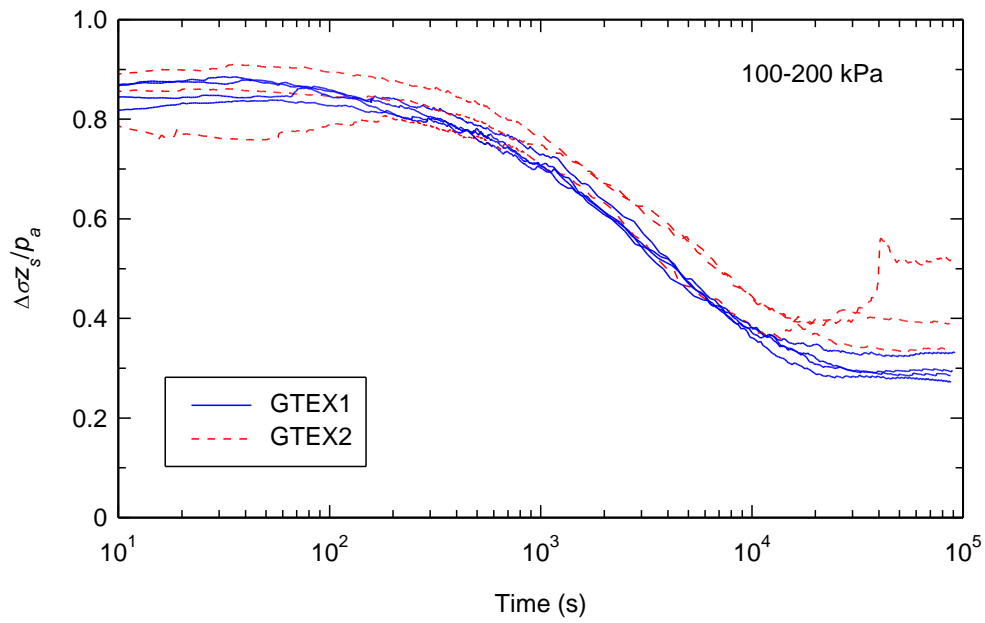


Figure 3. Normalized vertical stresses on the soil with time (encased columns).

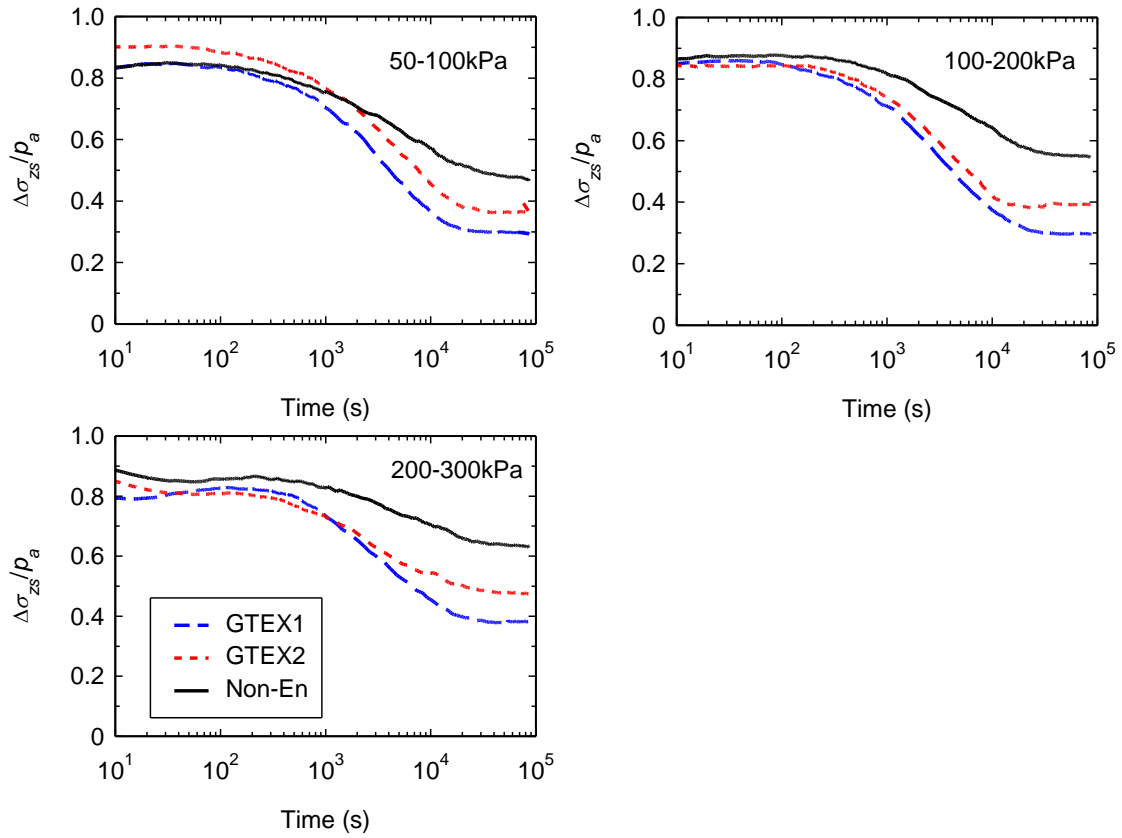


Figure 4. Normalized mean vertical stresses in the soil with time.

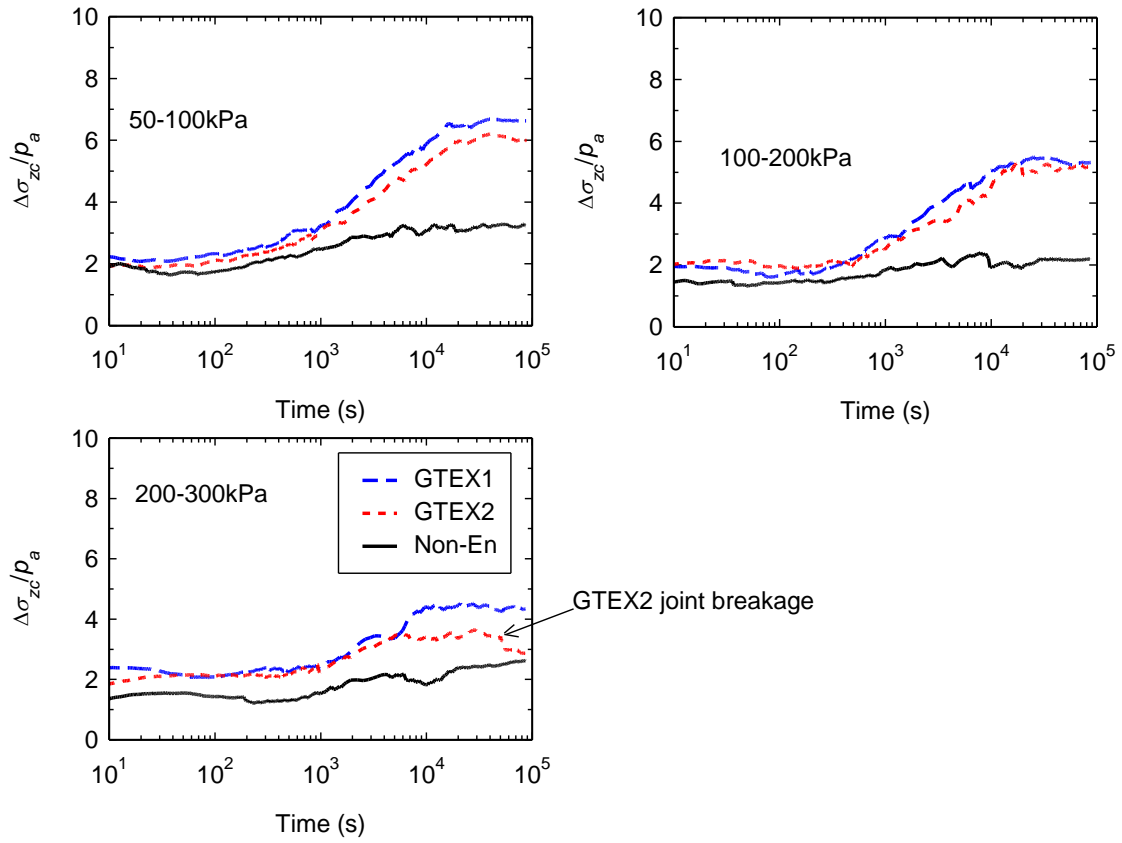


Figure 5. Normalized mean vertical stresses in the column with time.

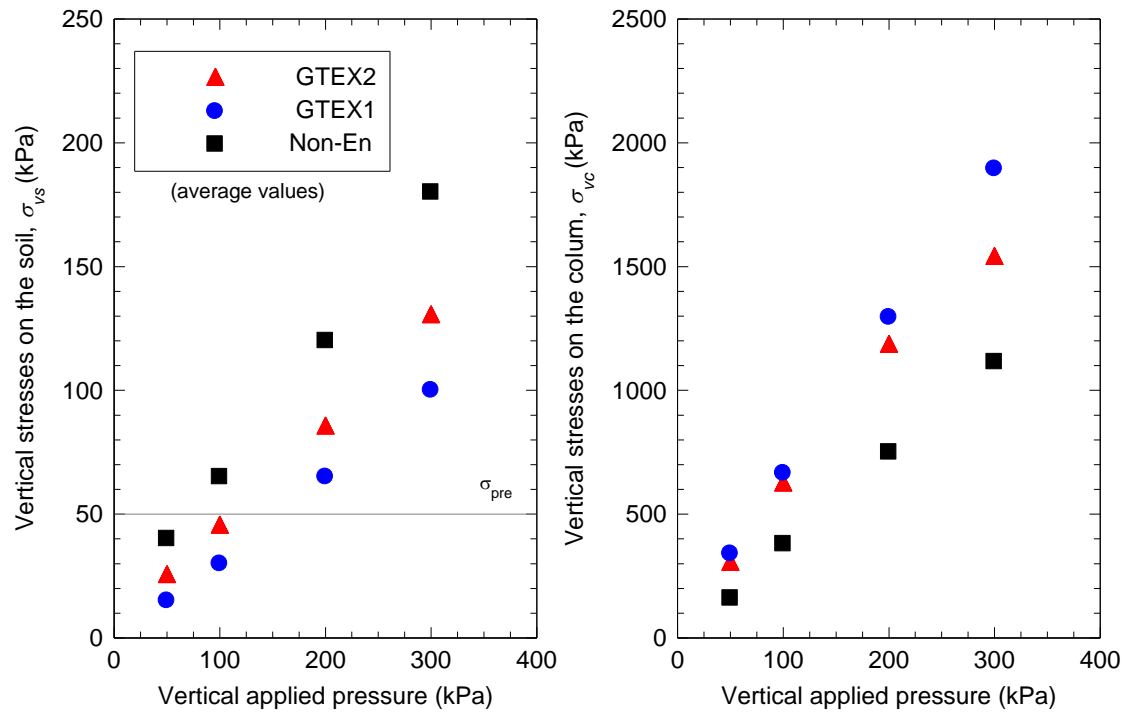


Figure 6. Vertical stresses on the soil and on the column under drained conditions.



Figure 7. Encased column with geotextile2 at the end of the test.

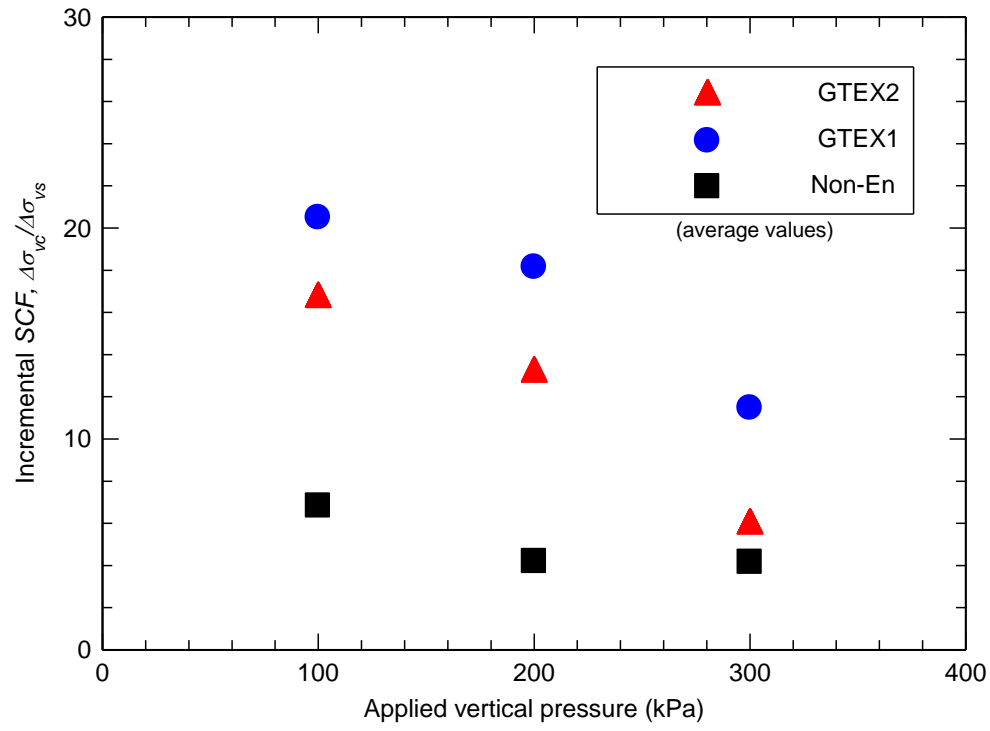


Figure 8. Incremental *SCF* in drained situation.

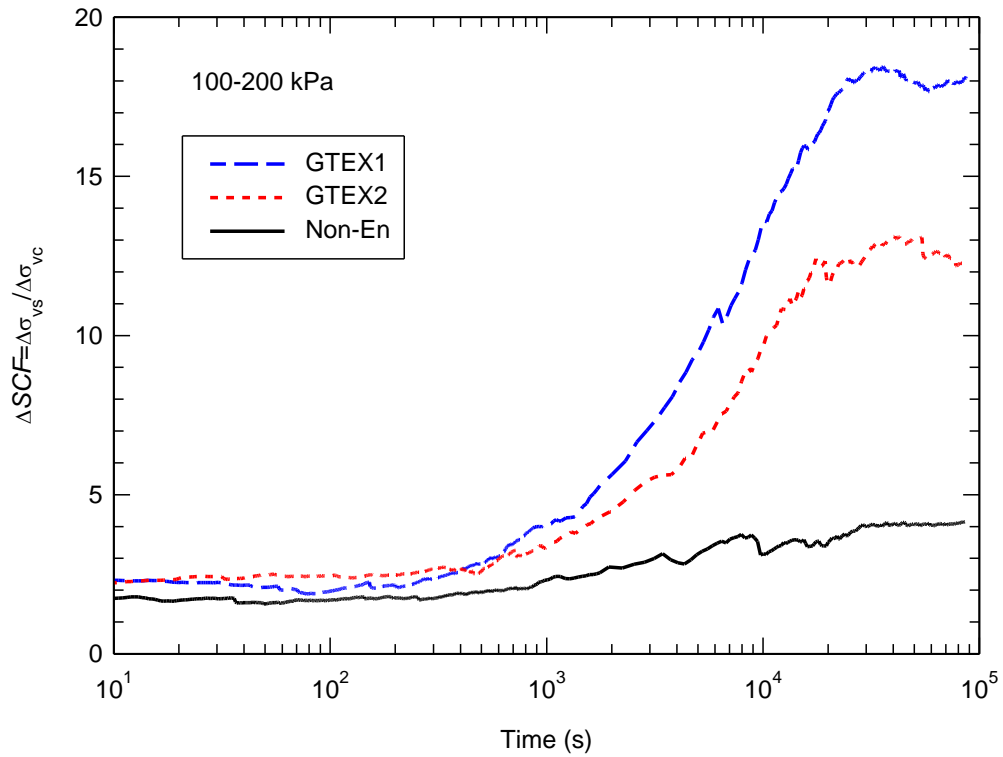


Figure 9. Incremental *SCF* with time for the three load steps.

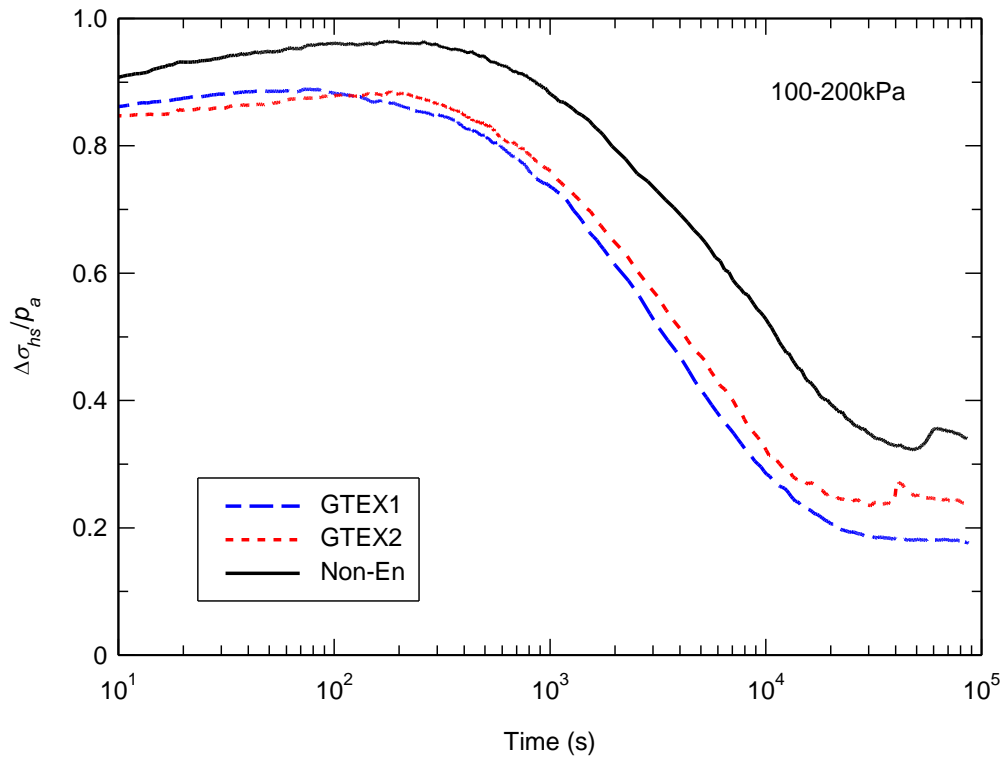


Figure 10. Horizontal stresses in the soil with time.

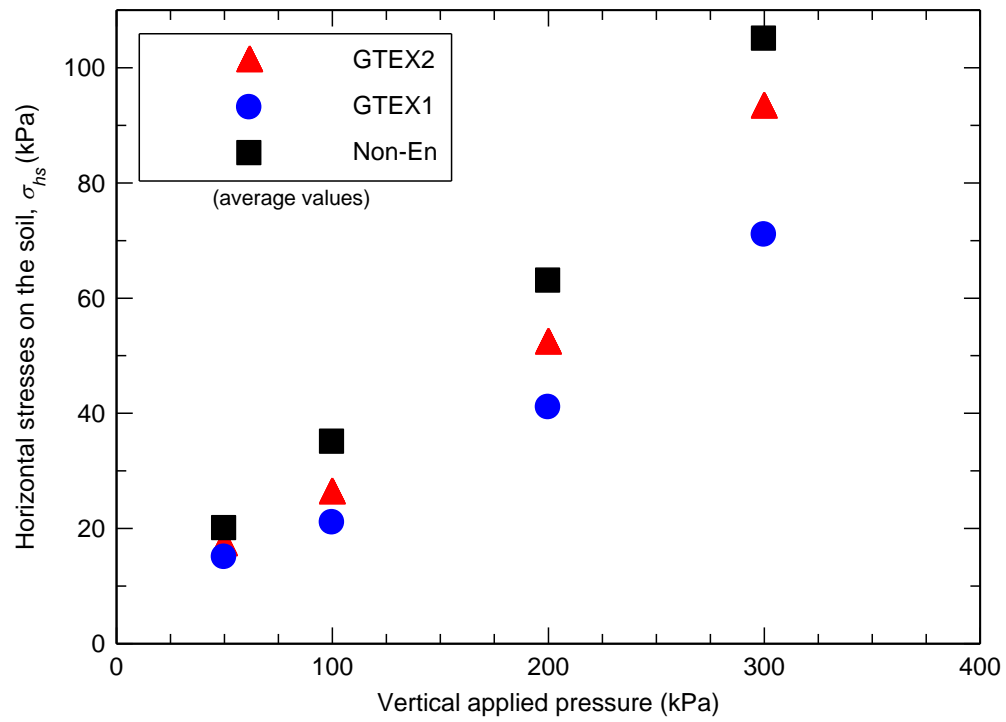


Figure 11. Horizontal stresses on the soil under drained conditions.

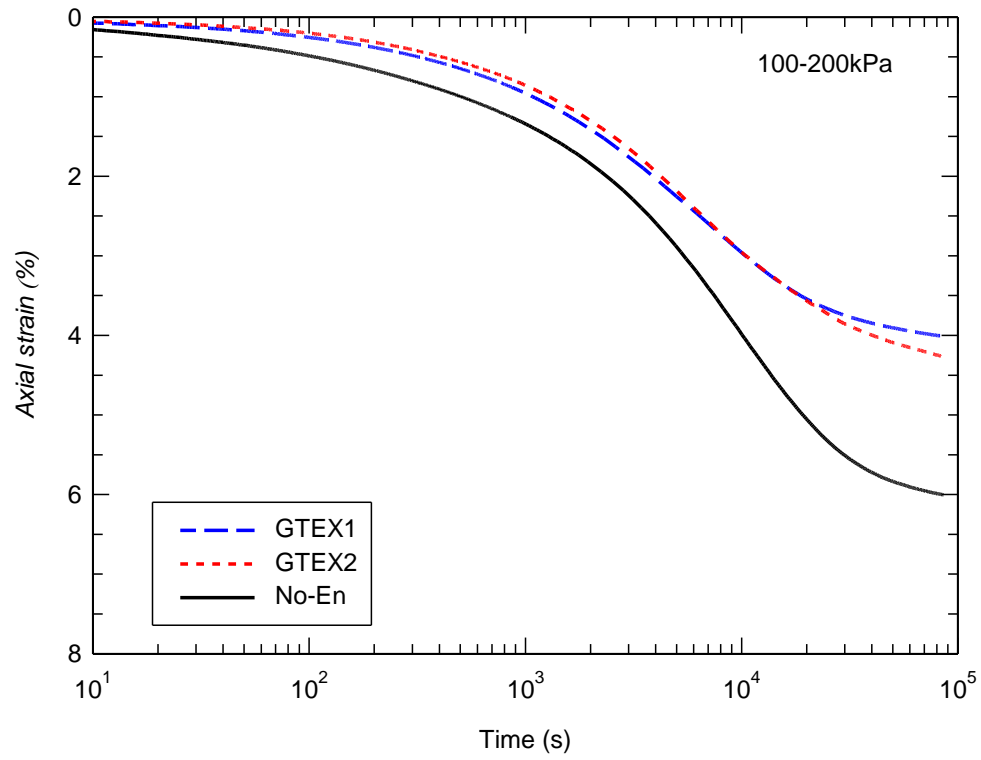


Figure 12. Axial strains with time.

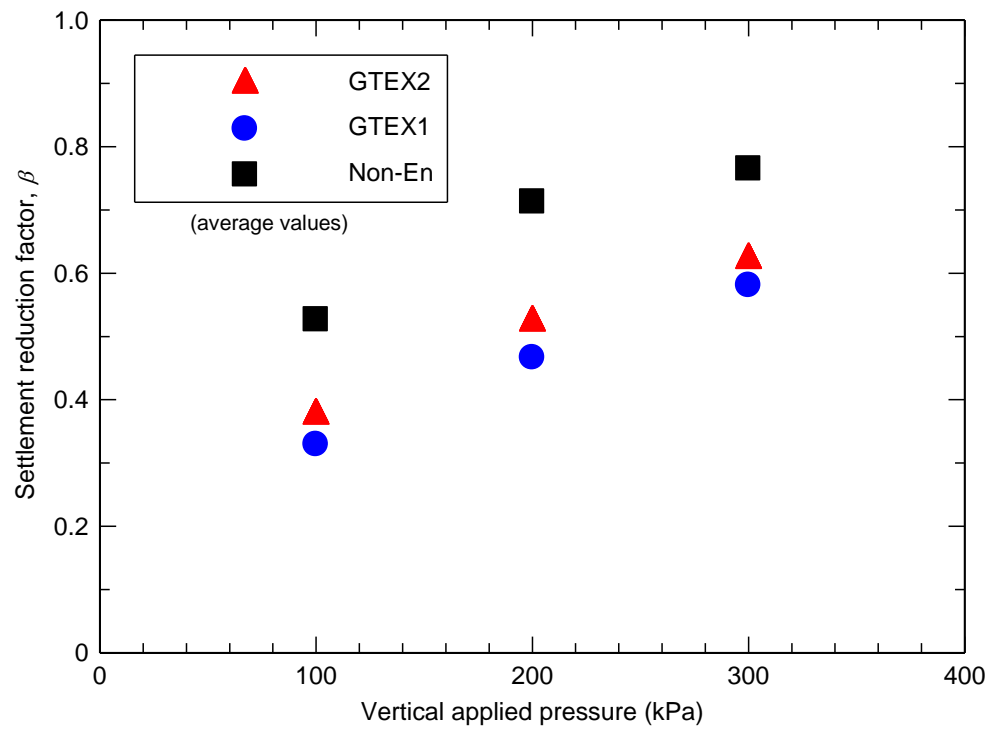


Figure 13. Settlement reduction factor at the end of each load step.

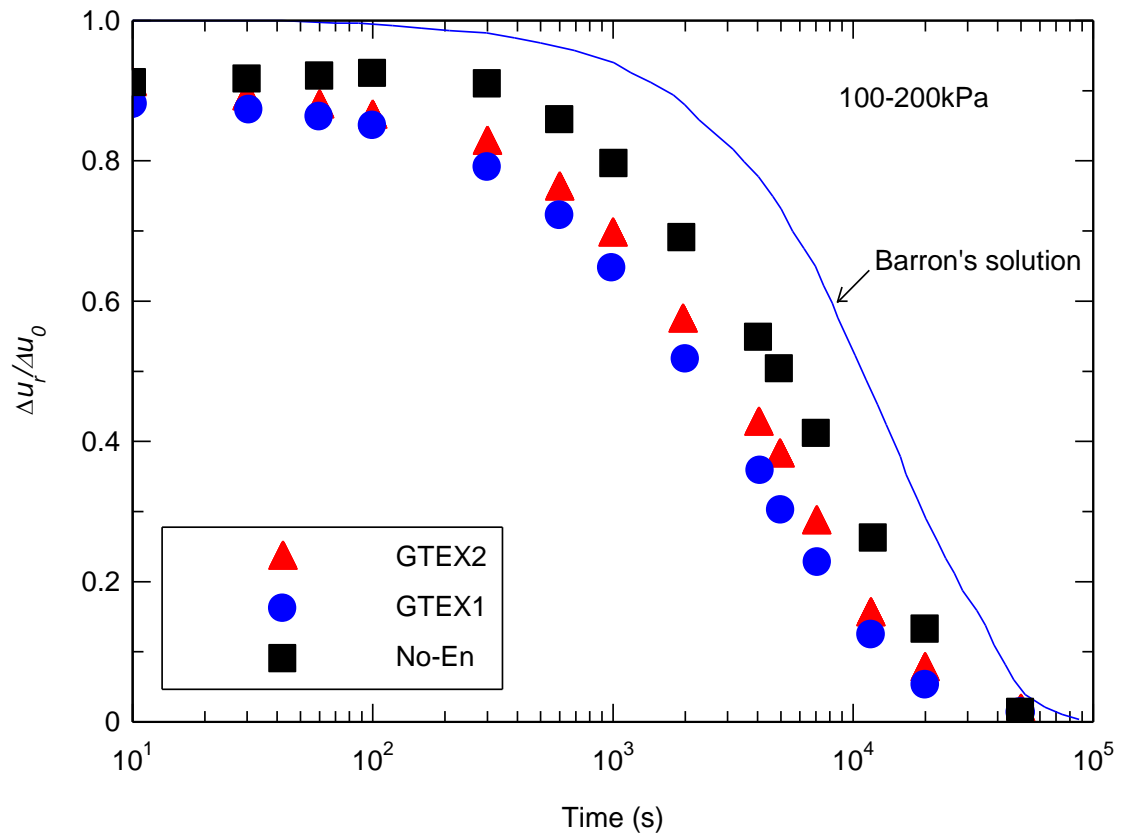


Figure 14. Pore pressure with time.

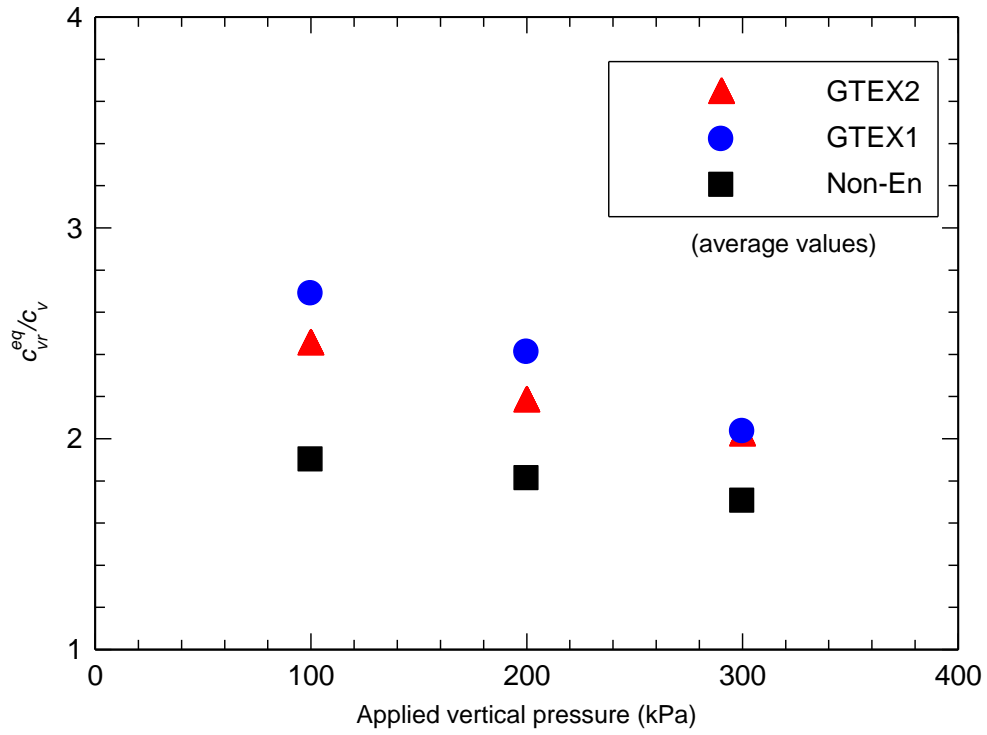


Figure 15. Equivalent coefficient of consolidation using Robinson (1997) method.